Chemical Engineering Journal 110 (2005) 113–121

Chemical Engineering Journal

www.elsevier.com/locate/cej

A factorial-design study of the variables affecting the electrochemical reduction of Cr(VI) at polyaniline-modified electrodes

Luís Augusto Martins Ruotolo *, José Carlos Gubulin

Department of Chemical Engineering, Federal University of São Carlos, P.O. Box 676, 13565-905 São Carlos, SP, Brazil

Received 9 September 2004; received in revised form 9 March 2005; accepted 11 March 2005

Abstract

An electrochemical process using reticulated vitreous carbon-supported polyaniline cathodes is proposed to reduce toxic hexavalent chromium, which is present in industrial wastewater. The effect of five variables was simultaneously studied: (1) flow velocity; (2) current density; (3) electrode thickness; (4) electrode porosity and (5) Cr(VI) concentration. Due to the number of variables, a Box–Behnken factorial-design was chosen in order to reduce the number of experiments required. The current efficiency, energy consumption and space–time yield were the variables evaluated. The process was also analyzed in terms of the polymer stability and the overpotential distribution inside the porous electrode.

Keywords: Hexavalent chromium; Conducting polymers; Reticulated vitreous carbon; Electrochemical engineering; Environmental electrochemistry

1. Introduction

In nature, chromium is found in two oxidation states: Cr(III) and Cr(VI). While hexavalent chromium is highly mobile in the environment, trivalent chromium is readily precipitated or adsorbed by a wide range of organic and inorganic substrates at neutral pH. Thus, immobilizing Cr(VI) by reducing it to Cr(III) facilitates effluent treatment [1]. Hexavalent chromium, usually found in wastewater of electroplating, electronic, metallurgical, leather tanning and textile industries, has been reported as being 10–100 times more toxic than Cr(III) [2]. Due to the toxic effects of hexavalent chromium and its environmental impact, Brazilian legislation (CETESB) sets the level of Cr(VI) permitted in wastewater at 0.1 mg L^{-1}.

Conventional processes for Cr(VI) reduction use chemical reagents, such as sulfur dioxide or sodium metabisulfite, that are consumed in the chemical reaction and cannot be recovered for reuse. The use of some of these reagents can also increase the volume of sludge generated. After Cr(VI) reduction, the Cr(III) is precipitated in the form of hydroxides and the sludge is dried and stored. In recent years, new methods to improve or substitute conventional processes have been developed. These include the use of gas diffusion electrodes [3], adsorptive processes [4–6] and the use of conducting polymer thin films [1,7–12]. In their reduced forms, conducting polymers can spontaneously transfer electrons to Cr(VI). The first conducting polymer used for this purpose was polypyrrole (PPY) in 1993 [1]. However, the loss of the electrochemical activity of polypyrrole to reduce Cr(VI) after consecutive cycles carried out under open circuit conditions has been reported [9]. This behavior has been attributed to polymer degradation. Ruotolo et al. [12] compared the kinetics of Cr(VI) reduction using polypyrrole and polyaniline films under open and closed circuit conditions. It was shown that polypyrrole is not suitable for use under either of the conditions due to polymer degradation. For polyaniline (PANI), open circuit condition cannot be considered as the polymer suffers complete degradation. However, when a potential lower than 0.6 V versus Ag/AgCl is applied in the range where polyaniline is stable, no degradation is observed after the reaction with Cr(VI). In addition, high reaction rates are observed, making the polyaniline film suitable

* Corresponding author. Tel.: +55 16 3351 8772; fax: +55 16 3351 8266.
E-mail address: luisruotolo@yahoo.com.br (L.A.M. Ruotolo).

1385-8947/$ – see front matter © 2005 Elsevier B.V. All rights reserved.
doi:10.1016/j.cej.2005.03.019

for use as an electrode material. In fact, Malinauskas and Holze [13] demonstrated that the contact between PANI and the Cr(VI) solution at open circuit conditions has the same effect as maintaining the polymer at very anodic potentials, where the PANI hydrolysis takes place with the main degradation product being *p*-benzoquinone [14]. Experiments using different polyaniline film thicknesses revealed that they have no influence on either the polymer stability or kinetics of Cr(VI) reduction, meaning that chromium reacts at the PANI/solution boundary [15]. Other results regarding the effect of the polymer on the kinetics of Cr(VI) reduction can be found in [11,12]. The strong electrocatalytic effect of polyaniline on Cr(VI) reduction has also been demonstrated [8].

In this light, PANI was chosen for this study in which a number of engineering variables were evaluated. Another factor that contributed to the choice of polyaniline was its ease of synthesis in aqueous medium and the low cost of the monomer. Reticulated vitreous carbon (RVC) was used as the substrate for PANI film deposition. The effect of five variables was simultaneously studied using the Box–Behnken factorial-design [16]. The variables studied were: (1) flow velocity; (2) current density; (3) electrode thickness; (4) electrode porosity and (5) Cr(VI) concentration. These parameters were chosen because they are directly related to both reactor and operational design. The efficiency of the process was evaluated by considering the current efficiency (CE) and energy consumption (EC), both of which are related to operational costs. The space–time yield was also calculated as it is directly related to capital costs. In order to understand better the electrochemical behavior inside the porous electrode, overpotential profiles were recorded.

2. Experimental

2.1. Preparation of RVC/PANI electrode

The polyaniline films were electrodeposited on the porous RVC substrates (12.7 mm thick, 40 mm wide and 70 mm long). Three different porosities were used: 30, 45 and 60 ppi (pores per inch). The RVC was furnished by the Electrosynthesis Company Inc., Buffalo, USA.

A flow cell composed of a current feeder, a separation mesh and a counter electrode (these materials are similar to those used in the reactor shown in Fig. 1) were used for PANI electrosynthesis.

The electrolyte containing 0.1 M of the aniline monomer (Mallinckrodt) in 1.0 M H_2SO_4 (Mallinckrodt) was passed through the reactor using a peristaltic pump. Potentiodynamic synthesis was performed within the potential limits of −0.1 and 0.8 V at a sweep rate of 50 mV s^{-1} [17]. For each of the electrodes with different porosities and specific surface areas, the electrosynthesis was performed until the current density peak reached the value of 0.2 mA cm^{-2} (always referring to the first anodic peak in the voltammogram). This procedure was used in order to obtain approximately the same film thickness characteristic for all the electrodes. In fact, due to the potential distribution inside the porous electrode, the polymer film thickness is not constant throughout the porous electrode thickness; however, Ruotolo and Gubulin [15] shown that the most important factor is to guarantee that all the RVC surface is covered, since the reaction of Cr(VI) will take place at the polyaniline/solution boundary.

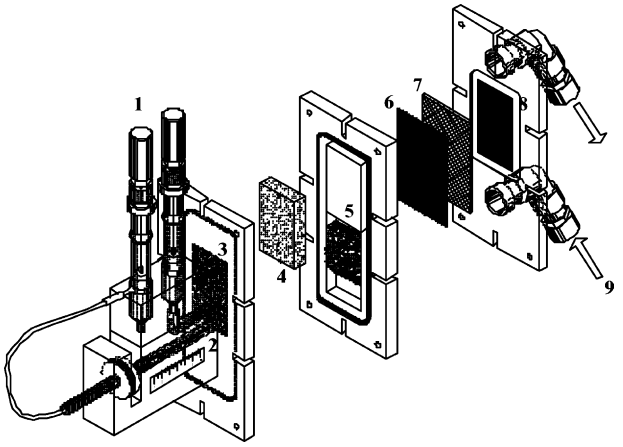

Fig. 1. Electrochemical reactor for galvanostatic reduction of Cr(VI). (1) Reference electrode; (2) mobile Luggin capillary; (3) current feeder; (4) RVC/PANI electrode; (5) flow distributor; (6) polyamide fabric; (7) polyethylene mesh; (8) counter electrode; (9) electrolyte inlet and outlet.

After electrosynthesis, the polyaniline film was washed with 1.0 M H_2SO_4 in order to eliminate monomer and oligomer residues. The freshly prepared electrode was then immediately used for Cr(VI) reduction.

All potentials are referred to the Ag/AgCl 3.0 M KCl reference electrode (207 mV versus SHE—standard hydrogen electrode).

2.2. Reaction of Cr(VI) reduction

A detailed view of the electrochemical reactor used for the reduction of Cr(VI) is presented in Fig. 1. The reactor was constructed in acrylic and the current feeder and the counter electrode both consisted of Ti/RuO_2 DSA® plates (De Nora, Sorocaba, Brazil). A polyethylene mesh, covered with polyamide fabric, was positioned between the anode and the cathode in order to avoid short circuits.

The experiments were carried out under galvanostatic conditions, without deoxygenation. Fig. 2 shows the setup used to perform these experiments. In order to avoid contact between the polyaniline film and the Cr(VI) solution under open circuit conditions, the current source was turned on before pumping the solution. Current control was achieved using a constant current source (Minipa—model 3003 D). The Cr(VI) concentration was recorded using an ULTROSPEC 2100pro UV–vis spectrophotometer (Amersham Pharmacia Biotech) equipped with a flow cubete and a peristaltic pump for “on line” concentration measurement at a wavelength of 350 nm. This method was used until the Cr(VI) concentration reach approximately 5.0 mg dm^{-3}. For

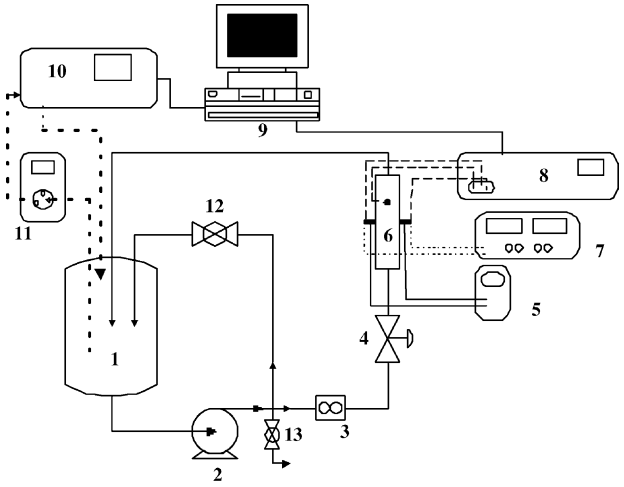

Fig. 2. Schematic view of the system used for Cr(VI) reduction. (1) Electrolyte reservoir; (2) centrifugal pump; (3) flow rate digital meter; (4) diaphragm valve; (5) voltmeter; (6) electrochemical reactor; (7) current source; (8) potentiostat; (9) computer; (10) UV–vis spectrophotometer; (11) peristaltic pump; (12) ball valve (by-pass); (13) ball valve (for electrolyte exhaustion).

lower concentrations, diphenylcarbazide (DFC) was used only for the qualitative detection of Cr(VI). The process finished when no more Cr(VI) could be detected by the DFC method. The voltage drop through the reactor was recorded using a digital multimeter and its mean value was used to calculate the energy consumption. In fact, there is only a small increase in the voltage drop during the experiment.

The electrode thickness was increased by simply joining together two or three of the 12.7 mm electrode and adding central pieces to the reactor shown in Fig. 2. The volume of electrolyte used was 4 dm^3 at an initial concentration of 100 mg dm^{-3} Cr(VI) ($K_2Cr_2O_7$, Merck, was used as source of hexavalent chromium). All reagents used were of analytical grade and all solutions were prepared using deionized water. The electrolyte temperature was maintained in the range of 25–28 °C.

2.3. Electrochemical responses of polyaniline

The electrochemical responses of the polyaniline films were recorded in 0.5 M H_2SO_4, before and after the reaction with Cr(VI). The potential range of −0.1 to 0.6 V and a sweep rate of 50 mV s^{-1} were used. By comparing the voltammograms obtained before and after the reaction, an estimate of the polymer stability could be made. The purpose here was to evaluate if the polymer remained stable under closed circuit conditions when subjected to the different current and flow velocities applied.

2.4. Overpotential profile measurements

The first step for overpotential determination was the rest potential measurement (potential at zero current). For that, a Cr(VI) reduction experiment was carried out by applying a constant current (chronopotentiometric method) and when the concentration reached the desired value (which was controlled by the coupled UV–vis spectrophotometer), the current source was turned off, so no external current was supplied for a few seconds (about 10 s) and the rest potential at that concentration was recorded by the potentiostat (EcoChemie, model PGSTAT30), which was coupled to the system shown in Fig. 1. This experiment was carried out in triplicate to ensure that the values of the rest potential were reproducible.

The potentials were recorded using the mobile Luggin capillary shown in Fig. 2 (item 2), which was coupled to a nut/screw system that enabled it to move inside the porous electrode. The capillary positions can be known exactly since they are a function of the screw step (1.5 mm). In these experiments the Luggin capillary was filled with a 3.0 M KCl solution whose viscosity was increased by adding agar–agar (6.5 g dm^{-3}) in order to avoid disturbances in potential measurement that can occasionally occur due to hydrodynamic turbulences.

Once the flow velocity and current density were established, the potential measurement procedure started. The potentiostat was only used to measure the potential profile, while an electric current source was used exclusively for current supply. When the desired concentration was reached (which could be verified on line by UV–vis) the potentiostat, set for chronopotentiometry in zero current mode, i.e., at open circuit condition (no current was applied by the potentiostat), was turned on and the Luggin capillary was moved inside the electrode. The capillary remained stationary for about 5 s in each of the desired positions. This was enough time to establish a steady potential, which corresponded exactly to the electrode potential at that specific capillary position. This procedure was necessary due to the fast rate of reaction. Also the electrolyte volume had to be increased to 10 dm^3 in order to guarantee that the change in Cr(VI) concentration during the recording of the potential profile (about 60 s) was insignificant.

The potential was recorded at 10 different positions along the direction of the electric field for the electrode of thickness of L = 12.7 mm (only for the electrode porosity of 60 ppi). The position $x/L = 0$ corresponded to the current feeder and $x/L = 1$ corresponded to the separation mesh. The profiles were expressed in terms of overpotential calculated by the difference between the potential and the rest potential at the same concentration.

2.5. Box–Behnken factorial-design

The Box–Behnken design [16] was chosen because it reduces the number of experiments necessary for a complete factorial-design (243 experiments!) and also because it allows the use of experimental conditions (variable levels), which would, for example, be prohibited in a central composite design. The former limitation is mainly due to the electrode porosity, which is commercially available in specific grades.

Table 1
Real and coded values of the variables used in the Box–Behnken experimental design

Variable	Coded values		
	−1	0	+1
v, flow velocity (m s^{-1})	0.09	0.12	0.15
I, current density (A m^{-2})	14.8	22.2	29.6
L, electrode thickness (mm)	12.7	25.4	38.1
ε, electrode porosity (ppi)	30	45	60
C, Cr(VI) concentration (mg dm^{-3})	10	55	100

The Box–Behnken experimental design consists basically of the classic two-level factorial-design (2^k, where k is the number of factors) increased by central points that permit the estimation of the second order coefficients. The variable codification, given by Eq. (1), follows the same procedure of the other factorial-design [16,18].

$$x_i = \frac{\zeta_i - \zeta_0}{\zeta_1 - \zeta_0} \tag{1}$$

x_i is the value of the coded variable (adimensional), ζ_i, ζ_0 and ζ_1 are the real values of the non coded variables (in their original dimension) corresponding to the non coded levels i, 0 and 1, respectively.

The levels (values) assumed by the five variables studied, as well as their coded values, are shown in Table 1. The Box–Behnken design codification is shown in Table A.1, in the Appendix A.

The values of flow velocity and current density were established based on preliminary tests and considering the electrode area of the different thickness and porosities of the RVC used. The electrode porosities were chosen taking in to account the values demanded by the Box–Behnken factorial-design and the commercial grades available. The choice of the different levels for the electrode thickness was made considering the commercial thickness available (12.7 mm). As many industries have problems with effluents containing low levels of Cr(VI), the initial concentration of 100 mg dm^{-3} was chosen for this work.

The evaluated responses were the current efficiency (CE), space–time yield ($Y_{s–t}$) and energy consumption (EC). The current efficiency, Eq. (2), is the ratio between the current effectively used for Cr(VI) reduction and the total current supplied. The energy consumption, Eq. (3), gives the energy used for the reduction of a mass unit of the compound. The space–time yield, Eq. (4), express the mass of reduced Cr(VI) as a function of time and reactor volume.

$$\mathrm{CE} = \frac{100 \cdot z \cdot F \cdot V}{M \cdot I} \cdot \left(-\frac{\mathrm{d}C}{\mathrm{d}t}\right) \tag{2}$$

CE is the current efficiency (%), dC/dt is the concentration drop in the time interval dt (g dm^{-3} s^{-1}), z the number of electrons used in the electrochemical reaction ($z = 3$ for reduction of Cr(VI) to Cr(III)), F the Faraday constant (96487 As mol^{-1}), I the electric current (A), V the electrolyte volume (dm^3) and M is the molar mass (51.996 g mol^{-1} for chromium).

$$\mathrm{EC} = \frac{2.78 \times 10^{-2} \cdot z \cdot F \cdot \Delta U}{\mathrm{CE} \cdot M} \tag{3}$$

EC is the energy consumption (kW h kg^{-1}) and ΔU is the voltage drop (V). The constant 2.78×10^{-2} has the unit h s^{-1}.

$$Y_{s–t} = \frac{\mathrm{CE} \cdot i \cdot A \cdot M}{10^5 \cdot z \cdot F \cdot V_R} \tag{4}$$

$Y_{s–t}$ is the space–time yield (kg s^{-1} m^{-3}), A the electrode surface area (m^2), i the current density (A m^{-2}) and V_R is the reactor volume (m^3).

3. Results and discussion

The current efficiency, energy consumption and space–time yield were calculated from the experimental curves of concentration and voltage drop (which increases during the process) as function of time (not shown) for each condition given by the experimental design (Table A.1—Appendix A). Eqs. (5)–(7) were fitted considering only the significant effects (confidence level above 95%) by the least squares method using the software Statistica 5.1.

$$\begin{aligned}\mathrm{CE} = {} & 57.1 - 30.9 \cdot i^{\mathrm{c}} - 42.6 \cdot L^{\mathrm{c}} - 20.6 \cdot \varepsilon^{\mathrm{c}} - 2.72 \cdot (\varepsilon^{\mathrm{c}})^2 \\ & + 45.5 \cdot C^{\mathrm{c}} + 19.0 \cdot (C^{\mathrm{c}})^2 - 18.6 \cdot L^{\mathrm{c}} \cdot C^{\mathrm{c}}\end{aligned} \tag{5}$$

$$\begin{aligned}Y_{s–t} = {} & 6.23 + 1.29 \cdot i^{\mathrm{c}} - 5.09 \cdot L^{\mathrm{c}} - 0.66 \cdot (L^{\mathrm{c}})^2 + 3.10 \cdot \varepsilon^{\mathrm{c}} \\ & + 4.89 \cdot C^{\mathrm{c}} + 1.89 \cdot (C^{\mathrm{c}})^2 - 2.15 \cdot i^{\mathrm{c}} \cdot L^{\mathrm{c}} \\ & - 2.30 \cdot L^{\mathrm{c}} \cdot \varepsilon^{\mathrm{c}} - 2.12 \cdot L^{\mathrm{c}} \cdot C^{\mathrm{c}}\end{aligned} \tag{6}$$

$$\begin{aligned}\mathrm{EC} = {} & 27.8 + 22.8 \cdot i^{\mathrm{c}} + 38.8 \cdot L^{\mathrm{c}} - 7.0 \cdot \varepsilon^{\mathrm{c}} + 7.9 \cdot (\varepsilon^{\mathrm{c}})^2 \\ & - 34.0 \cdot C^{\mathrm{c}} - 14.2 \cdot (C^{\mathrm{c}})^2 + 19.9 \cdot i^{\mathrm{c}} \cdot L^{\mathrm{c}} \\ & - 15.7 \cdot i^{\mathrm{c}} \cdot C^{\mathrm{c}} - 20.1 \cdot L^{\mathrm{c}} \cdot C^{\mathrm{c}}\end{aligned} \tag{7}$$

The regression coefficients (R^2) for CE, $Y_{s–t}$ and EC were 0.9001, 0.92339 and 0.91623, respectively. At a confidence level of 95% the values of R^2 are acceptable considering the nature of the experimental design, which covers a large number of variables. The plot of residual versus fitted values (not shown) was sufficiently random, i.e. no evident tendencies were observed, consequently no variable transformation was required and the model adopted in Eqs. (5)–(7) is appropriate.

The flow velocity is curiously absent in Eqs. (5)–(7), meaning that it does not influence the reduction process. Analyzing only the effect of flow velocity in Table A.1, it can be observed that when the flow velocity is increased, a small increase in current efficiency is also observed for most runs. However, when compared with the effect of the other variables studied, the effect of flow velocity, statistically speaking, becomes negligible. This indicates that the increase in

the mass transfer coefficient within the narrow range of velocities studied is not enough to cause an important change in CE, Y_{s-t} and EC.

The surface response methodology was used for the analysis of the variables and their interactions affecting the process responses. This method consist of representing the response graphically in a three-dimensional space and it is especially useful for modeling and analysis of problems in which a response of interest is influenced by several variables and the objective is to optimize this response [18]. For the surfaces shown, the levels of the factors not plotted were maintained in their intermediate value (i.e., zero). Except for certain conditions, the increase or decrease in these levels only displaced the response surface downward or upward, but did not change the surface morphology.

3.1. Current efficiency

Fig. 3a shows current efficiency as a function of current density and electrode thickness (both coded). Increasing the electrode thickness, the drop of CE as a function of i^c remains linear, but their values decrease. There is a drop in CE when the current density increases, which is a consequence of the existence of parallel reactions. This effect becomes more important when the electrode thickness is increased. In fact, the existence of an overpotential profile explains these observations and this will be discussed later.

The electrode porosity was not observed to have an important effect on the CE, as only a small increase was observed when the value of ε was reduced.

The current efficiency is largely influenced by the Cr(VI) concentration, as shown in Fig. 3b. When working in galvanostatic mode, the current efficiency reduction over the process is due to the transition from kinetic to mass control [15]. At low concentrations, mass transfer becomes important and limits the reaction rate. As the concentration is lowered, the hydrogen evolution reaction becomes more important and the current efficiency decreases.

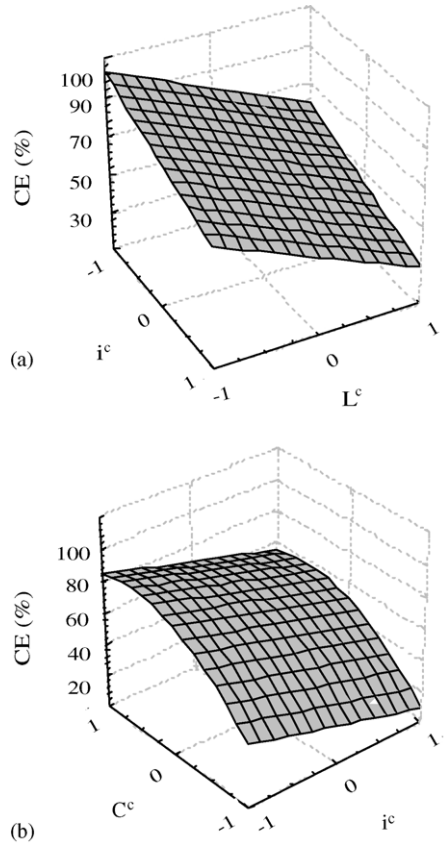

Fig. 3. (a) Current efficiency as function of i^c and L^c, $v^c = 0$, $\varepsilon^c = 0$, $C^c = 0$; (b) current efficiency as function i^c and C^c, $v^c = 0$, $L^c = 0$, $\varepsilon^c = 0$.

3.2. Space–time yield

The space–time yield was especially useful for the evaluation of the effect of electrode thickness as it permits an analysis of the reaction rate (kg s^{-1}) per unit of electrode volume (m^3). Initially, only the reaction rates were considered for analysis and an increase in their values was observed when the electrode thickness was increased. This behavior was expected since more current should be furnished in order to provide the same current density and consequently the reaction rates also increase. However, when the electrode thickness was doubled, the reaction rate did not double. Because of this fact, it was decided to use the space–time yield for an effective analysis of the electrode thickness on the process, since the effect of current efficiency is also taken in account when working with Y_{s-t}.

Fig. 4 shows that when the electrode thickness increases, Y_{s-t} also increases, especially at the high current densities, but this increase is not proportional since for high current densities there is a drop of the current efficiency (Fig. 3a). Considering the effect of ε^c, Fig. 5, it is demonstrated that increasing the number of pores per inch of the electrode (i.e. increasing its surface area) there is an increase in Y_{s-t}. However, when the electrode thickness is increased, Fig. 5b, the capacity of the current density and electrode porosity to cause an increase in the space–time yield drops. For the electrode

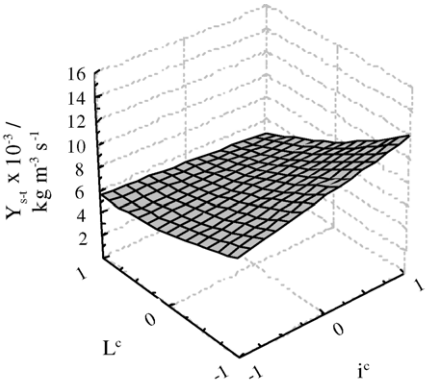

Fig. 4. Space–time yield as function of i^c and L^c, $v^c = 0$, $\varepsilon^c = 0$, $C^c = 0$.

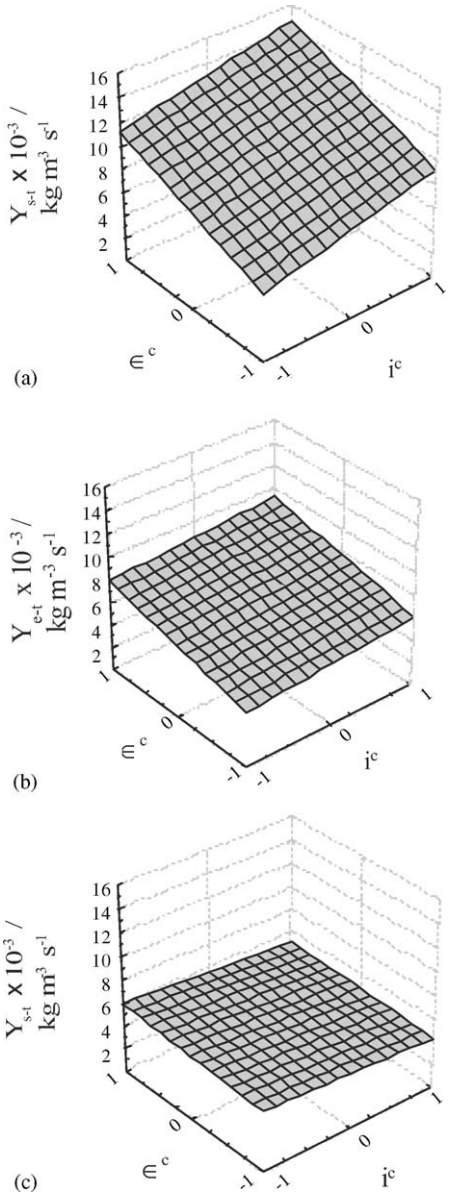

Fig. 5. Space–time yield as function of i^c and ε^c, $v^c = 0$ and $C^c = 0$. (a) $L^c = -1$; (b) $L^c = 0$ and (c) $L^c = +1$.

thickness of 38.1 mm ($L^c = +1$, Fig. 5c) Y_{s-t} is almost constant and is practically independent of the current density and porosity. This behavior can be explained remembering that to calculate the space–time yield from Eq. (4) we have to consider only the current effectively used in the Cr(VI) reaction (i.e. the product of current density and current efficiency ($i \times$ CE)). When the current density and the surface area increase, the current supplied is increased too; however, at the same time the current efficiency decreases (see Fig. 3a). For thin electrodes, the product $i \times$ CE increases as well as the charge supplied and the space–time yield is little affected by the current efficiency as the CE drop is not very sharp (Fig. 3a and b). However, for thicker electrodes, CE sharply decreases and consequently Y_{s-t} decreases. For the electrode thickness of 38.1 mm ($L^c = +1$), CE decreases in the same proportion

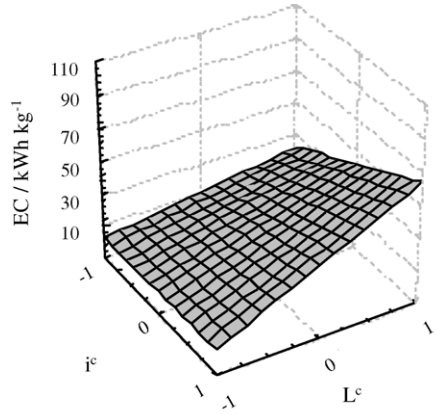

Fig. 6. Energy consumption as function of i^c and L^c, $v^c = 0$, $\varepsilon^c = 0$, $C^c = 0$.

as the current increases and the constant behavior shown in Fig. 5c is explained.

The effect of Cr(VI) concentration on the space–time yield presents the same behavior shown in Fig. 3b for CE. As Y_{s-t} is directly proportional to CE, when the latter decreases following the concentration drop, the same occurs with Y_{s-t}.

3.3. Energy consumption

The energy consumption is a direct function of current efficiency and voltage drop (Eq. (3)), thus the behavior of the surface shown in Fig. 6 has to be understood by taking in to account these two variables. When the electrode thickness is increased, a sharp decrease in current efficiency and the increase in voltage drop make the process display high values of energy consumption and the process becomes unfeasible from an economic point of view. For the electrode thickness of 12.7 mm ($L^c = -1$), the decrease of CE and the increase of the voltage drop were not very important considering the current efficiency and the energy consumption remained practically constant. However, when the concentration drops, the energy consumption increases due mainly to the decrease of the current efficiency.

The electrode porosity has little influence on EC; however, when ε is increased a small increase in energy consumption is verified. This probably occurs because the effective electrolyte conductivity is affected by the electrode porosity when the number of pores per inch increases [19]. The greater the ppi grade electrode the smaller the effective conductivity and consequently the energy consumption increase.

The electrolyte concentration plays the same role for energy consumption as for current efficiency, i.e., when the concentration is very low, the energy consumption becomes prohibitive. Also an increase in the voltage drop is observed when the Cr(VI) concentration decreases, which also contributes to an increase in EC.

3.4. Overpotential profiles

In order to understand better some of the results obtained in the statistical study, Fig. 7a and b present some

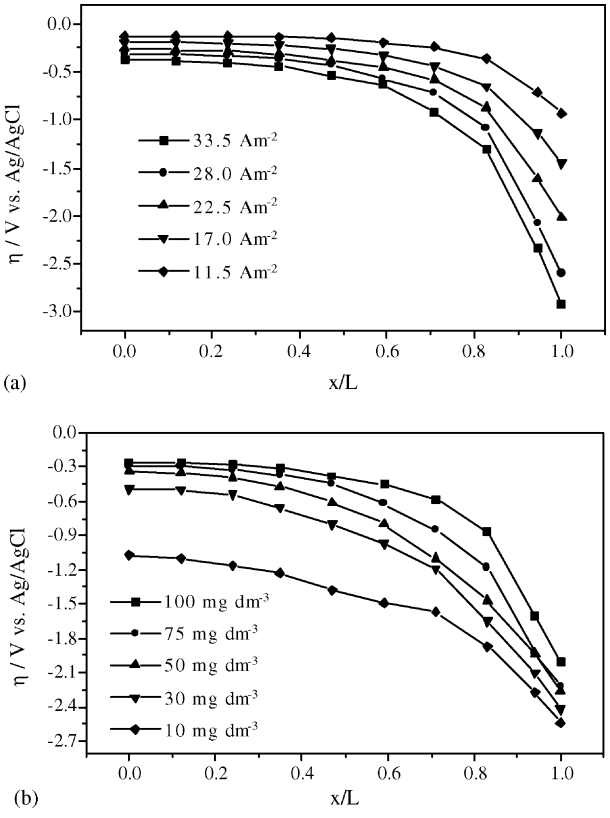

Fig. 7. Overpotential profiles for the RVC/PANI electrode. (a) Current density as the parameter; (b) Cr(VI) concentration as the parameter. Flow velocity: 0.15 m s^{-1}; L = 12.7 mm.

overpotential profiles recorded at the RVC/PANI electrode (L = 12.7 mm). A variation in the electrochemical activity can be observed along the electrode thickness. The spontaneous capacity of polyaniline as an electron donor for Cr(VI) reduction was not able to eliminate or reduce the extent of low reaction rate zones inside the electrode (lower negative overpotential values).

The most active portion of the electrode is concentrated in the region next to the counter electrode (x/L = 1), representing about only 40% of the total electrode thickness. Perhaps, thinner electrodes would simultaneously optimize the reaction rate variables and the electrode cost.

Increasing the current density (Fig. 7a) the overpotentials become more and more negative and consequently the reaction rate also increases. However, the overpotential values are not uniform and they start to be very negative close to the counter electrode and in this region the hydrogen evolution reaction competes with Cr(VI) reduction and consequently the current efficiency will drop. In this light it can be explained why the increase in the electrode thickness from 12.7 to 25.4 mm and 38.1 mm makes the process operate at very low current efficiencies. In order to obtain the same current density when the electrode thickness is increased, more current must be supplied. However, due to the non uniformity effect of the overpotential profiles, this extra current will tend to concentrate close to the counter electrode [20]. As this charge is not used for Cr(VI) reduction due to limitations imposed by mass transfer, more and more charge will be diverted to the hydrogen evolution reaction, which is favored by the very negative overpotentials in this region. Consequently the sharp decrease in current efficiency shown in Fig. 3a occurs when the electrode thickness is increased.

Concerning the concentration, Fig. 7b shows that the lower the concentration the more negative the overpotentials and the same discussion presented in the former paragraph can be applied. When the concentration drops, more negative potential regions form and mass transfer again controls the kinetics of Cr(VI) reduction. At the same time hydrogen evolution makes the current efficiency to decrease (see Fig. 3b). In fact, using a mathematical model to fit the overpotential profiles (not shown) for the concentrations of 10, 30 and 50 mg dm^{-3}, the limiting current kinetic (mass transfer control) was adequate to describe the experimental result shown in Fig. 7b [19].

3.5. Stability of the RVC/PANI electrode

Polyaniline degradation was not detected within the range of values of the variables studied. This is demonstrated by the fact that the voltammograms for polyaniline films in all experiments were practically identical when compared before and after the reaction with Cr(VI), meaning that the closed circuit condition is efficient in avoiding polymer degradation during chromium(VI) reduction. Even for a six-hour experiment, no losses in the electrochemical activity of the polyaniline were observed, as verified from the voltammograms, so leaching of the polymer also does not occur. In fact, as can be seen from the potential profiles (not shown, but it can be estimated from Fig. 7a, subtracting 0.71 V, which is the rest potential for 100 mg dm^{-3}), no potential greater than 0.6 V versus Ag/AgCl was verified, consequently, no polymer degradation was detected.

4. Conclusions

The influence of operational parameters on Cr(VI) reduction at polyaniline-modified electrodes has been investigated and the results have shown that:

(i) Increasing the current density supplied for the electrode of 12.7 mm, there is an increase in the space–time yield, but at the same time the current efficiency drops and energy consumption increases. This suggests that an optimum operational condition exists with a 100% CE, lower ECs and consequently an optimized Y_{s-t}.

(ii) An increase in the number of pores per inch of the electrode is desirable since it greatly increases the electrode surface, permitting that more current to be supplied for the same electrode volume (greatly increasing Y_{s-t}). It will also increase the hydrodynamic turbulence

increasing the mass transfer and favouring the Cr(VI) reduction.

(iii) Increasing the electrode thickness did not increase the process efficiency. The negative effects associated with an increase of the electrode thickness, such as CE and Y_{s-t} reduction and EC growth outweigh the benefits of the reaction rate increase observed. This is due to the fact that the major part of the current concentrates only in a region close to the counter electrode.

(iv) The depletion in Cr(VI) concentration as a function of time is very important for the operational optimization of this electrochemical process. Current control as function of Cr(VI) concentration has to be developed in order to avoid the sharp decrease of CE and Y_{s-t} and the increase in EC observed for all conditions studied.

Acknowledgement

This research was supported by FAPESP (São Paulo State Research Aid Foundation, Brazil) under Project Number 99/10.822-9.

Appendix A

See Table A.1.

Table A.1
The Box–Behnken experimental design

Runs	v^c	i^c	L^c	ε^c	C^c	CE (%)	Y_{s-t} (kg m^{-3} s^{-1})	EC (kW h kg^{-1})
1	−1	−1	0	0	0	79.4	6.02	12.7
2	1	−1	0	0	0	92.0	6.97	9.4
3	−1	1	0	0	0	44.2	6.69	33.5
4	1	1	0	0	0	47.9	7.25	28.1
5	0	0	−1	−1	0	96.5	7.07	4.8
6	0	0	1	−1	0	78.8	4.99	16.5
7	0	0	−1	1	0	89.8	13.8	6.9
8	0	0	1	1	0	46.5	7.16	37.1
9	0	−1	0	0	−1	36.8	2.79	27.0
10	0	1	0	0	−1	20.0	3.04	73.7
11	0	−1	0	0	1	96.5	7.31	9.4
12	0	1	0	0	1	57.2	8.66	24.7
13	−1	0	−1	0	0	100	11.3	5.8
14	1	0	−1	0	0	100	11.3	5.7
15	−1	0	1	0	0	35.2	4.01	49.4
16	1	0	1	0	0	38.5	4.39	41.9
17	0	0	0	−1	−1	24.9	1.82	43.7
18	0	0	0	1	−1	30.0	4.62	35.4
19	0	0	0	−1	1	90.6	6.64	11.6
20	0	0	0	1	1	62.4	9.62	16.2
21	0	0	0	0	0	66.8	7.59	20.3
22	0	0	0	0	0	59.4	6.75	21.1
23	0	0	0	0	0	56.4	6.41	21.3
24	0	−1	−1	0	0	100	7.88	4.2
25	0	1	−1	0	0	83.9	12.71	9.2
26	0	−1	1	0	0	55.8	4.24	23.3
27	0	1	1	0	0	31.4	4.76	67.9
28	−1	0	0	−1	0	76.6	5.61	13.9
29	1	0	0	−1	0	92.1	6.75	10.0
30	−1	0	0	1	0	53.3	8.21	22.5
31	1	0	0	1	0	59.5	9.17	19.2
32	0	0	−1	0	−1	29.1	3.31	23.3
33	0	0	1	0	−1	21.2	2.41	98.7
34	0	0	−1	0	1	94.3	10.72	5.6
35	0	0	1	0	1	49.1	5.59	40.8
36	−1	0	0	0	−1	23.6	2.68	62.1
37	1	0	0	0	−1	20.5	2.33	59.3
38	−1	0	0	0	1	56.4	6.41	24.7
39	1	0	0	0	1	63.3	7.20	17.7
40	0	−1	0	−1	0	99.0	4.84	7.0
41	0	1	0	−1	0	59.3	5.79	18.4
42	0	−1	0	1	0	69.7	7.14	12.6
43	0	1	0	1	0	41.9	8.60	32.5
44	0	0	0	0	0	62.8	7.14	21.6
45	0	0	0	0	0	64.8	7.37	19.3
46	0	0	0	0	0	63.8	7.25	18.8

Note: The superscript c indicates the variable value at its coded form. Results for CE, Y_{s-t} and EC.

References

[1] C. Wei, S. German, S. Basak, K. Rajeshwar, Reduction of hexavalent chromium in aqueous solutions by polypyrrole, J. Electrochem. Soc. 140 (1993) L60–L62.

[2] D.E. Kimbrough, Y. Cohen, A.M. Winer, L. Creelman, C. Mabuni, A critical assessment of chromium in the environment, Crit. Rev. Environ. Sci. Tech. 29 (1999) 1–46.

[3] K.N. Njau, L.J.J. Janssen, Electrochemical reduction of chromate ions from dilute artificial solutions in a GBC-reactor, J. Appl. Electrochem. 29 (1999) 411–419.

[4] M.P. Candela, J.M.M. Martinez, R.T. Macia, Chromium(VI) removal with activated carbons, Water Res. 29 (1995) 2174–2180.

[5] D. Petruzzelli, R. Passino, G. Tiravanti, Ion exchange process for chromium removal and recovery from tannery wastes, Ind. Eng. Chem. Res. 34 (1995) 2612–2617.

[6] I. Han, M.A. Schlautman, B. Batchelor, Removal of hexavalent chromium from groundwater by granular activated carbon, Water Environ. Res. 72 (2000) 29–39.

[7] R. Senthurchelvan, Y. Wang, S. Basak, K. Rajeshwar, Reduction of hexavalent chromium in aqueous solutions by polypyrrole, J. Electrochem. Soc. 143 (1996) 44–51.

[8] A. Malinauskas, R. Holze, An in situ spectroelectrochemical study of redox reactions at polyaniline-modified ITO electrodes, Ber. Bunsenges. Phys. Chem. 102 (1998) 982–984.

[9] M.A. Alatorre, S. Gutierrez, U. Paramo, J.G. Ibanez, Reduction of hexavalent chromium by polypyrrole deposited on different carbon substrates, J. Appl. Electrochem. 28 (1998) 551–557.

[10] J.R. Rodrigues, S. Gutierrez, J.G. Ibanez, J.L. Bravo, N. Batina, The efficiency of toxic chromate reduction by a conducting polymer (polypyrrole): influence of electrodeposition conditions, Environ. Sci. Technol. 34 (2000) 2018–2023.

[11] L.A.M. Ruotolo, J.C. Gubulin, Reduction of hexavalent chromium using polyaniline films. Effect of film thickness, potential and flow velocity on the reaction rate and polymer stability, J. Appl. Electrochem. 33 (2003) 1217–1222.

[12] L.A.M. Ruotolo, A.A. Liao, J.C. Gubulin, Reaction rate and electrochemical stability of conducting polymer films used for the reduction of hexavalent chromium, J. Appl. Electrochem. 34 (2004) 1259–1263.

[13] A. Malinauskas, R. Holze, In situ UV–vis spectroelectrochemical study of polyaniline degradation, J. Appl. Polym. Sci. 73 (1999) 287–294.

[14] C.Q. Cui, X.H. Su, J.Y. Lee, Measurement and evaluation of polyaniline degradation, Polym. Degrad. Stab. 41 (1993) 69–76.

[15] L.A.M. Ruotolo, J.C. Gubulin, Chromium(VI) reduction using conducting polymer films, React. Funct. Polym. 62 (2005) 141–151.

[16] G.E.P. Box, D.W. Behnken, Some new three level designs for the study of quantitative variables, Technometrics 2 (1960) 455–475.

[17] W.S. Huang, B.D. Humphrey, A.G. MacDiarmid, Polyaniline, a novel conducting polymer, J. Chem. Soc. Faraday Trans. I 82 (1986) 2385–2400.

[18] D.C. Montgomery, Design and Analysis of Experiments, third ed., John Wiley & Sons, USA, 1991.

[19] L.A.M. Ruotolo, J.C. Gubulin, Reduction of hexavalent chromium using polyaniline films. Overpotential profiles inside the RVC/PANI electrode, in: Proceedings of the 30th Brazilian Congress of Parti culated Systems, São Carlos, Brazil, 2002.

[20] L.A.M. Ruotolo, J.C. Gubulin, Electrodeposition of copper íons on fixed bed electrodes: kinetic and hydrodynamic study, Braz. J. Chem. Eng. 19 (2002) 108–118.